



CrossMark
click for updates

Cite this: *RSC Adv.*, 2015, 5, 37512

Received 8th February 2015

Accepted 9th April 2015

DOI: 10.1039/c5ra02461g

www.rsc.org/advances

A microfluidic-based controllable synthesis of rolled or rigid ultrathin gold nanoplates†

Qiang Fu,^{ab} Guangjun Ran^a and Weilin Xu^{*a}

A continuous, microfluidic-based, seed-mediated synthesis of high-purity gold nanoplates with different thicknesses was developed. The thickness of the nanoplates can be fairly tuned from less than 1 nm to a few nm by varying the flow rate. Depending on the thickness, the obtained nanoplates could be rigid and flat-surfaced with thicknesses larger than 2 nm or flexible with crumpled or rolled shapes when the thickness is around 1 nm. These nanoplates are poly-crystalline with different crystal faces and show high electrochemical activity towards glucose oxidation.

Introduction

The control of metal nanostructure morphology (size, shape, and surface structure) has attracted considerable attention in recent years due to the interest in precise tuning of electronic, optical, and catalytic properties.^{1–4} Consequently, a variety of nonspherical gold nanocrystals with different shapes such as rods,^{5,6} wires,^{7,8} belts,^{9,10} combs,¹⁰ plates and prisms,^{11,12} polyhedra,^{13–17} cages and frames,¹⁸ caps,¹⁹ stars and flowers,^{20–24} as well as dendrites^{25–29} have been achieved. However, these varied types of nanocrystals were obtained by bench top batch preparative methods, which are successful in the laboratory. These methods are not convenient for the synthesis of anisotropic nanocrystals on a large scale. Therefore, microfluidic methods have been regarded as suitable alternative protocols with a high probability of continuously gaining large quantities of particles with a uniform size and shape.^{30,31} Moreover, among the gold nanocrystals discussed above, microfluidic protocols have been used to prepare various shapes of nanoparticles with different sizes (*e.g.* spherical nanoparticles, nanorods, and hexagonal and triangular nanoplates).^{30,32–39} As for gold nanoplates, to the best of our knowledge, no one has already successfully prepared gold nanoplates with different thickness by the microfluidic protocol, although a similar protocol has been used for the synthesis of different-sized gold nanoparticles.³⁶ Although various bench top batch preparative methods have been reported for the synthesis of gold nanoplates with or without a bending contour,^{12,40–42} these gold nanoplates mainly have sizes in the micrometer range and

thicknesses of tens of nanometers, with mixed shapes including obtuse triangles, hexagons, and quasi-rounds. Furthermore, the evitable production of a large number of ball-like nanoparticles during these preparations is really a waste of gold sources, which are limited on the earth.

Recently, we reported a continuous microfluidic-based synthesis of Au supraparticles.⁴³ In that work, it was revealed that a type of flexible, thin Au nanoplate is in fact the first intermediate for the growth of Au supraparticles. Herein, by varying the flow rate in the microfluidic device, we obtained a series of Au nanoplates with controllable thickness and found that the morphology (rolled or rigid) of the Au nanoplates could be tuned by controlling the thickness of the nanoplates. In addition, the electrochemical test shows that the electrocatalytic activity of the nanoplates toward glucose oxidation depends on the morphology of the nanoplates: the rolled ones show considerably higher catalytic activity than the flat ones.

Experimental section

Chemicals

Hydrogen tetrachloroaurate trihydrate ($\text{HAuCl}_4 \cdot 3\text{H}_2\text{O}$) was purchased from Sigma-Aldrich. Cetyltrimethylammonium chloride (CTAC), sodium borohydride (NaBH_4), and ascorbic acid (AA) were purchased from Shanghai Sinopharm Chemical Reagent Co., Ltd. Sodium bromide (NaBr), β -D-glucose, sulphuric acid (H_2SO_4), and potassium hydrogen phosphate (KH_2PO_4 and K_2HPO_4) were purchased from Beijing Chemical Co. All chemicals were used as received without further purification. Ultrapure distilled water ($18.2 \text{ M}\Omega \text{ cm}$) was used for all solution preparations.

Synthesis of gold seeds

10 mL aqueous solution containing $2.5 \times 10^{-4} \text{ M HAuCl}_4$ and 0.10 M CTAC was prepared first. Then, 0.45 mL of the NaBH_4 solution (0.02 M, ice-cold) was added into the above mentioned

^aState Key Laboratory of Electroanalytical Chemistry, Jilin Province Key Laboratory of Low Carbon Chemical Power, Changchun Institute of Applied Chemistry, Chinese Academy of Science, 5625 Renmin Street, Changchun 130022, P. R. China. E-mail: weilinxu@ciac.ac.cn

^bGraduate University of Chinese Academy of Science, Beijing, 100049, China

† Electronic supplementary information (ESI) available. See DOI: 10.1039/c5ra02461g

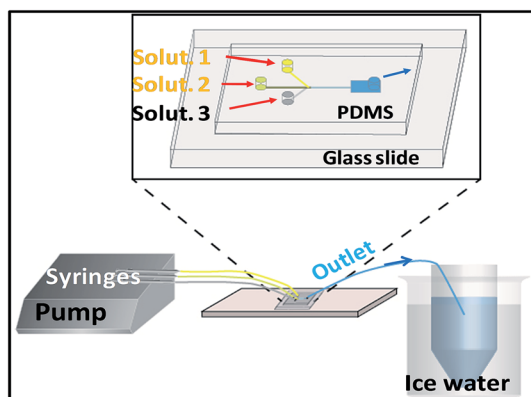
solution with stirring. The resulting solution turned brown immediately, indicating the formation of gold seeds, which were aged for 1 h at 30 °C to decompose excess borohydride. The seed particles have a size of about 4 nm (Fig. S1†).

Microfluidic synthesis of gold nanoplate

The microfluidic chip consists of a microchannel (400 μm \times 400 μm cross-section and 3 cm long) with three inlets and one outlet.⁴³ As shown in Scheme 1 and Fig. S2,† the reaction regime was divided into three different solutions: solution 1: 375 μL of 0.01 M HAuCl_4 solution, 15 μL of 0.01 M NaBr solution and 4.6 mL of 0.1 M CTAC solution were mixed together; solution 2: 135 μL of 0.04 M ascorbic acid solution and 4.8 mL of 0.1 M CTAC solution were added together; and solution 3: 150 μL seed solution and 4.8 mL of 0.1 M CTAC solution were added together. Then, these three different solutions were injected into the microfluidic chip through three independent channels at the same rate. Moreover, the effluent from the chip was collected into a centrifugal tube with a large amount of ice-cold ultrapure water to terminate the growth. The solution in the tube was then centrifuged at 12 000 rpm for at least 15 min. To remove the excess surfactant, the precipitate was washed by water twice through centrifugation at 12 000 rpm for not less than 15 min. By varying the flow rate of the solution, nanoplates with different thicknesses were obtained.

Preparation of the gold nanoplate-modified electrode

A glassy carbon electrode (GCE) was polished before each experiment with 1, 0.3 and 0.05 μm alumina slurry and then successively washed with diluted nitric acid, acetone and distilled water in an ultrasonic bath. The original solution containing nanoplates (*ca.* 15 mL) was concentrated to 1 mL, and then 100 μL of the condensed solution was dropped onto the pretreated GCE and dried in the air. After that, 4 μL Nafion (0.1%) was cast onto the electrode. Such a modified electrode was used for electrochemical characterization. The modified electrode was stored at 4 °C when not in use.



Scheme 1 The setup of the flow-based microfluidic system for synthesis of the ultrathin gold nanoplate.

Instrumentation

UV-vis absorption spectra were taken using a JASCO V-570 spectrophotometer. Transmission electron microscopy (TEM), high resolution transmission electron microscopy (HRTEM) and selected area electron diffraction (SAED) characterization was performed using JEOL JEM-2100 electron microscopes with an operating voltage of 200 kV. Digital HRTEM images were analyzed to determine the crystallinity of the nanoplates using a digital micrograph 3.7. Atomic force microscopy (AFM) images were generated with a Veeco Multimodel NanoScope 3D in the tapping AFM mode. All electrochemical experiments were performed using a CHI 750E electrochemical workstation (CH Instruments, Chenhua Co., Shanghai, China). A conventional three-electrode system was employed with a modified GCE (3.0 mm in diameter) as working electrode, a platinum sheet as auxiliary electrode and a saturated calomel electrode (SCE) as reference electrode.

Results and discussion

First, the sample of folded or rolled nanoplate is prepared at 70 $\mu\text{L min}^{-1}$ based on our previous report. The detailed morphology of the sample was characterized as before.⁴³ Fig. 1a and S3(a–e)† show clearly that the well-defined nanoplates are rolled or folded to different extents. In addition, a thickness of about 1 nm could be predominantly seen from the rolled edge of the nanoplate (Fig. S3b†). The HRTEM image of an individual nanoplate (Fig. 1b) displays clear lattice fringes with fringe spacing of about 0.235 nm, indicating that the entire nanoplate is crystalline with the (111) facet running across the main surface of the nanoplate. The SAED pattern (Fig. 1c) shows a set

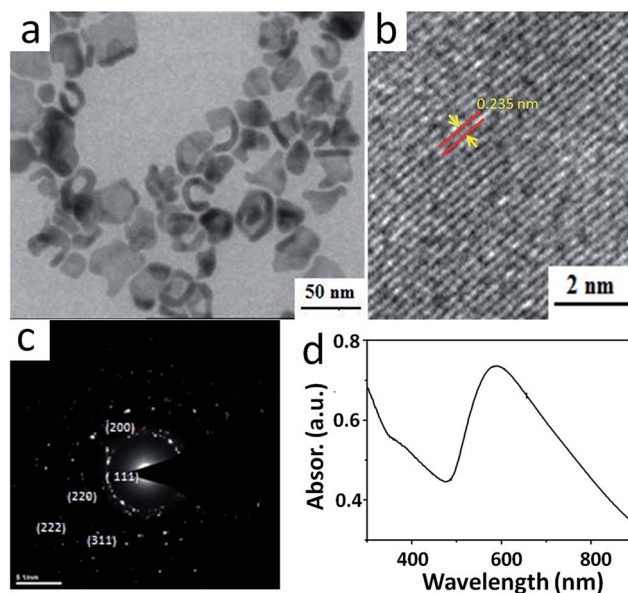


Fig. 1 (a) Typical TEM image of rolled Au nanoplates. (b) Typical HRTEM image of the surface of a Au nanoplate shown in (a). (c) Correlated SAED pattern for sample shown in (a). (d) Absorption spectra of ultrathin crumpled gold nanoplates shown in (a).

of diffraction spots indexed to the (111), (200), (220), (311) and (222) reflections of the gold fcc structure. The UV-vis spectrum (Fig. 1d) shows a relatively narrow absorption band with the maximum absorption at about 590 nm, revealing that rolled nanoplates have a relatively uniform size.⁴⁰

Furthermore, to investigate the mechanism of such a rapid growth process, a series of microfluidic experiments at different flow rates were performed (data shown in Fig. S4†). To our surprise, it can be concluded that the rolled ultrathin gold nanoplates mentioned before can be obtained at a relatively high flow rate, whereas at a low rate, the rigid, flat-surfaced nanoplates could be obtained. Fig. 2a and b show that the products acquired at $5 \mu\text{L min}^{-1}$ are just the rigid nanoplates with the fringe spacing of 0.235 nm (indexed to the (111) facet), which is consistent with that of the rolled nanoplate shown in Fig. 1b. Atomic force microscopy (AFM) was utilized to certify the thickness of rigid nanoplates. As shown in Fig. 2c and d, the thickness of the nanoplates obtained with a flow rate of $5 \mu\text{L min}^{-1}$ is about 5.5 nm, which is considerably thicker than that ($<1 \text{ nm}$) prepared at $70 \mu\text{L min}^{-1}$ mentioned above (HRTEM image shown in Fig. S3b†). Moreover, the sample gained at $5 \mu\text{L min}^{-1}$ is thicker than the flat-surfaced sample (with thickness $\sim 2.5 \text{ nm}$) prepared at $10 \mu\text{L min}^{-1}$ (Fig. S5†). In addition, AFM was used to characterize the samples prepared at 30 and $50 \mu\text{L min}^{-1}$. Unfortunately, the exact height of rolled nanoplates cannot be measured directly by AFM due to their complicated rolling mode (Fig. S6†). Based on these facts, we can conclude that, when the flow rate is low, the nanoplates could grow thick due to a long growth time before they flowed out from the chip and then were quenched by the iced water in the tube shown in Scheme 1. As the flow rate increases, the growth time decreases, which then leads to thinner Au nanoplates. When they are thin enough, they tend to roll up to reduce the high surface energy.

Glucose oxidation in a phosphate buffered electrolyte is used to produce electricity in fuel cells, and similar experimental conditions are adopted here to evaluate the electrocatalytic activities of different gold nanoplates. Before that, GCEs modified by the rolled (red curve) and rigid (black curve)

nanostructures were tested in $0.5 \text{ M H}_2\text{SO}_4$. As shown in Fig. 3a, the cyclic voltammetry (CV) curves show that the rolled nanoplate (obtained with flow rate of $70 \mu\text{L min}^{-1}$) modified electrode displays a considerably higher peak current, which is associated with surface oxide reduction events, than that of the rigid ones. Therefore, it is expected that the rolled nanoplates may show a better performance in electrochemical oxidation of glucose than the rigid flat-surfaced nanoplates. Fig. 3b shows CV curves for glucose oxidation in a phosphate buffered solution on these two modified GCEs. Two main regions can be observed. The first peak is at 0.2 V vs. SCE , an oxidation peak (peak A, which cannot be seen clearly in the rolled nanoplate modified GCE), which is assigned to the dehydrogenation of the anomeric carbon of the glucose molecule. The current corresponding to this process is higher for rolled nanoplates than rigid ones. This dehydrogenation leads to the formation of gluconolactone. The second peak presents the main oxidation peak centered at around 0.3 V vs. SCE (peak B), which corresponds to the further oxidation of gluconolactone.^{44,45} Compared with that of the rigid nanoplate modified GCE, the rolled nanoplate modified GCE exhibited considerably larger oxidation currents, which clearly demonstrate the better electrocatalytic activity of the rolled nanoplates towards the glucose oxidation than the rigid ones. Moreover, the electrocatalytic activities of gold nanoplates prepared at $10 \mu\text{L min}^{-1}$, $30 \mu\text{L min}^{-1}$ and $50 \mu\text{L min}^{-1}$ were evaluated. As shown in Fig. S7,† their electrocatalytic activity is between that of rigid nanoplates (prepared at $5 \mu\text{L min}^{-1}$) and rolled nanoplates (prepared at $70 \mu\text{L min}^{-1}$). In addition, their electrocatalytic activity is increased with increasing flow rate (shown in Fig. S7†).

Moreover, the electrodeposition method is one of the most useful approaches to prepare various types of gold nanostructures such as nanorods,^{46,47} nanocubes⁴⁸ and spherical nanoparticles.⁴⁹ Nanoparticles with different shapes and sizes can be facilely synthesized on the conducting surfaces by altering the conditions of electrochemical deposition. It is beneficial to synthesize the hybrid material.^{50–52} The isolated nanoparticle has to be acquired by an additional separation process.⁴⁶ As for the microfluidic-based method, a higher surface to volume ratio and a lower sample consumption enable the chemical reaction processing in a continuous model to be completed within a short time and give a relatively uniform reaction environment.^{35–39} Moreover, microfluidic protocols

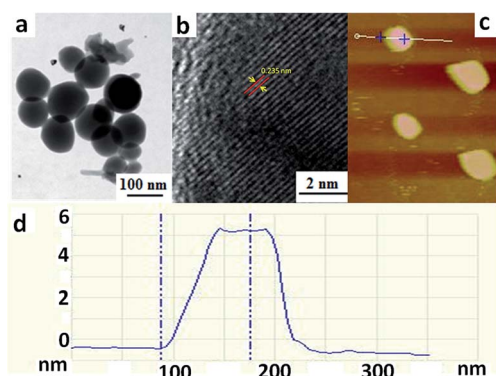


Fig. 2 (a) Typical TEM image of flat-surfaced Au nanoplates prepared at the rate of $5 \mu\text{L min}^{-1}$, (b) typical HRTEM image of the surface of a nanoplate shown in (a), (c) typical AFM image of sample shown in (a), and (d) height profile along the colored line of a rigid gold nanoplate shown in (c).

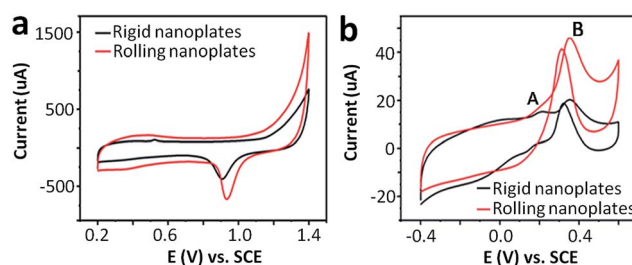


Fig. 3 (a) The cyclic voltammograms of two types of (rigid/rolled) nanoplate modified electrodes in (a) $0.5 \text{ M H}_2\text{SO}_4$, (b) in PBS (pH 7.4) in the presence of 10 mM glucose recorded at 50 mV s^{-1} and at $20 \text{ }^\circ\text{C}$.

offer the capability to automate a multi-step synthesis with less human operation.

Conclusions

We have developed a continuous seed-mediated method for the preparation of high-purity gold nanoplates with tunable thickness, which are rolled or rigid depending on their sizes. These nanoplates are poly-crystalline with different crystal faces and show a high electrochemical activity toward glucose oxidation. This protocol is fast, reproducible and adaptable to microfluidic synthesis without any additional batch processing steps and probably could be extended to the synthesis of other types of ultrathin nanoplates.

Acknowledgements

This work was funded by the National Basic Research Program of China (973 Program, 2012CB932800 and 2014CB932700), the National Natural Science Foundation of China (21273220 and 21422307), and “the Recruitment Program of Global youth Experts” of China.

References

- 1 Y. Xia and N. J. Halas, *MRS Bull.*, 2005, **30**, 338–348.
- 2 C. J. Murphy, *Science*, 2002, **298**, 2139–2141.
- 3 P. V. Kamat, *J. Phys. Chem. B*, 2002, **106**, 7729–7744.
- 4 M. A. El-Sayed, *Acc. Chem. Res.*, 2001, **34**, 257–264.
- 5 N. R. Jana, L. Gearheart and C. J. Murphy, *Adv. Mater.*, 2001, **13**, 1389.
- 6 B. Nikoobakht and M. A. El-Sayed, *Chem. Mater.*, 2003, **15**, 1957–1962.
- 7 C. Wang and S. Sun, *Chem.–Asian J.*, 2009, **4**, 1028–1034.
- 8 H. Feng, Y. Yang, Y. You, G. Li, J. Guo, T. Yu, Z. Shen, T. Wu and B. Xing, *Chem. Commun.*, 2009, 1984–1986.
- 9 J. Zhang, J. Du, B. Han, Z. Liu, T. Jiang and Z. Zhang, *Angew. Chem., Int. Ed.*, 2006, **45**, 1116–1119.
- 10 N. Zhao, Y. Wei, N. Sun, Q. Chen, J. Bai, L. Zhou, Y. Qin, M. Li and L. Qi, *Langmuir*, 2008, **24**, 991–998.
- 11 R. Jin, Y. Cao, C. A. Mirkin, K. Kelly, G. C. Schatz and J. Zheng, *Science*, 2001, **294**, 1901–1903.
- 12 A. Miranda, E. Malheiro, E. Skiba, P. Quaresma, P. A. Carvalho, P. Eaton, B. de Castro, J. A. Shelnutt and E. Pereira, *Nanoscale*, 2010, **2**, 2209–2216.
- 13 F. Kim, S. Connor, H. Song, T. Kuykendall and P. Yang, *Angew. Chem., Int. Ed.*, 2004, **43**, 3673–3677.
- 14 D. Seo, C. I. Yoo, J. C. Park, S. M. Park, S. Ryu and H. Song, *Angew. Chem., Int. Ed.*, 2008, **47**, 763–767.
- 15 G. H. Jeong, M. Kim, Y. W. Lee, W. Choi, W. T. Oh, Q. H. Park and S. W. Han, *J. Am. Chem. Soc.*, 2009, **131**, 1672–1673.
- 16 C. Li, K. L. Shuford, M. Chen, E. J. Lee and S. O. Cho, *ACS Nano*, 2008, **2**, 1760–1769.
- 17 M. S. Yavuz, W. Li and Y. Xia, *Chem.–Eur. J.*, 2009, **15**, 13181–13187.
- 18 S. E. Skrabalak, J. Chen, Y. Sun, X. Lu, L. Au, C. M. Copley and Y. Xia, *Acc. Chem. Res.*, 2008, **41**, 1587–1595.
- 19 N. Zhao, L. Li, T. Huang and L. Qi, *Nanoscale*, 2010, **2**, 2418–2423.
- 20 H.-G. Liao, Y.-X. Jiang, Z.-Y. Zhou, S.-P. Chen and S.-G. Sun, *Angew. Chem., Int. Ed.*, 2008, **47**, 9100–9103.
- 21 P. S. Kumar, I. Pastoriza-Santos, B. Rodriguez-Gonzalez, F. J. G. de Abajo and L. M. Liz-Marzan, *Nanotechnology*, 2008, **19**, 015606.
- 22 S. Barbosa, A. Agrawal, L. Rodríguez-Lorenzo, I. Pastoriza-Santos, R. n. A. Alvarez-Puebla, A. Kornowski, H. Weller and L. M. Liz-Marzán, *Langmuir*, 2010, **26**, 14943–14950.
- 23 P. R. Sajanlal and T. Pradeep, *Nano Res.*, 2009, **2**, 306–320.
- 24 Z. Wang, J. Zhang, J. M. Ekman, P. J. Kenis and Y. Lu, *Nano Lett.*, 2010, **10**, 1886–1891.
- 25 Y. Qin, Y. Song, N. Sun, N. Zhao, M. Li and L. Qi, *Chem. Mater.*, 2008, **20**, 3965–3972.
- 26 T. Huang, F. Meng and L. Qi, *Langmuir*, 2009, **26**, 7582–7589.
- 27 X. Xu, J. Jia, X. Yang and S. Dong, *Langmuir*, 2010, **26**, 7627–7631.
- 28 W. Ye, J. Yan, Q. Ye and F. Zhou, *J. Phys. Chem. C*, 2010, **114**, 15617–15624.
- 29 H. HianáTeo, *Chem. Commun.*, 2010, **46**, 7112–7114.
- 30 S. E. Lohse, J. R. Eller, S. T. Sivapalan, M. R. Plews and C. J. Murphy, *ACS Nano*, 2013, **7**, 4135–4150.
- 31 D. Kumar, A. Kulkarni and B. Prasad, *Colloids Surf., A*, 2014, **443**, 149–155.
- 32 C. Bullen, M. J. Latter, N. J. D'Alonzo, G. J. Willis and C. L. Raston, *Chem. Commun.*, 2011, **47**, 4123–4125.
- 33 V. Sebastián, S.-K. Lee, C. Zhou, M. F. Kraus, J. G. Fujimoto and K. F. Jensen, *Chem. Commun.*, 2012, **48**, 6654–6656.
- 34 J. Boleininger, A. Kurz, V. Reuss and C. Sönnichsen, *Phys. Chem. Chem. Phys.*, 2006, **8**, 3824–3827.
- 35 C.-H. Weng, C.-C. Huang, C.-S. Yeh, H.-Y. Lei and G.-B. Lee, *J. Micromech. Microeng.*, 2008, **18**, 035019.
- 36 V. Sebastian Cabeza, S. Kuhn, A. A. Kulkarni and K. F. Jensen, *Langmuir*, 2012, **28**, 7007–7013.
- 37 L. L. Lazarus, A. S.-J. Yang, S. Chu, R. L. Brutchey and N. Malmstadt, *Lab Chip*, 2010, **10**, 3377–3379.
- 38 D. Shalom, R. C. Wootton, R. F. Winkle, B. F. Cottam, R. Vilar and C. P. Wilde, *Mater. Lett.*, 2007, **61**, 1146–1150.
- 39 J. Wagner and J. M. Köhler, *Nano Lett.*, 2005, **5**, 685–691.
- 40 S. Yang, T. Zhang, L. Zhang, S. Wang, Z. Yang and B. Ding, *Colloids Surf., A*, 2007, **296**, 37–44.
- 41 Y. Shao, Y. Jin and S. Dong, *Chem. Commun.*, 2004, 1104–1105.
- 42 B. Cao, B. Liu and J. Yang, *CrystEngComm*, 2013, **15**, 5735–5738.
- 43 Q. Fu, Y. Sheng, H. Tang, Z. Zhu, M. Ruan, W. Xu, Y. Zhu and Z. Tang, *ACS Nano*, 2015, **9**, 172–179.
- 44 M. Pasta, F. La Mantia and Y. Cui, *Electrochim. Acta*, 2010, **55**, 5561–5568.
- 45 J. Wang, J. Gong, Y. Xiong, J. Yang, Y. Gao, Y. Liu, X. Lu and Z. Tang, *Chem. Commun.*, 2011, **47**, 6894–6896.
- 46 B. M. I. van der Zande, M. R. Böhmer, L. G. J. Fokkink and C. Schönenberger, *Langmuir*, 2000, **16**, 451–458.
- 47 B. M. Van der Zande, M. R. Böhmer, L. G. Fokkink and C. Schönenberger, *J. Phys. Chem. B*, 1997, **101**, 852–854.

- 48 J. Hernández, J. Solla-Gullón, E. Herrero, A. Aldaz and J. M. Feliu, *J. Phys. Chem. C*, 2007, **111**, 14078–14083.
- 49 H. Zhang, J.-J. Xu and H.-Y. Chen, *J. Phys. Chem. C*, 2008, **112**, 13886–13892.
- 50 J. C. Claussen, M. M. Wickner, T. S. Fisher and D. M. Porterfield, *ACS Appl. Mater. Interfaces*, 2011, **3**, 1765–1770.
- 51 Y. Hu, J. Jin, P. Wu, H. Zhang and C. Cai, *Electrochim. Acta*, 2010, **56**, 491–500.
- 52 A. D. Franklin, D. B. Janes, J. C. Claussen, T. S. Fisher and T. D. Sands, *Appl. Phys. Lett.*, 2008, **92**, 013122.